WANG, S., FERNANDEZ, C., FAN, Y., FENG, J., YU, C., HUANG, K. and XIE, W. 2020. A novel safety assurance method based on the compound equivalent modeling and iterate reduce particle-adaptive Kalman filtering for the unmanned aerial vehicle lithium ion batteries. *Energy science and engineering* [online], 8(5), pages 1484-1500. Available from: https://doi.org/10.1002/ese3.606

A novel safety assurance method based on the compound equivalent modeling and iterate reduce particle-adaptive Kalman filtering for the unmanned aerial vehicle lithium ion batteries.

WANG, S., FERNANDEZ, C., FAN, Y., FENG, J., YU, C., HUANG, K., XIE, W.

2020

Received: 17 September 2019 | Revised: 10 December 2019 | Accepted: 11 December 2019

DOI: 10.1002/ese3.606

Energy Science & Engineering
Open Access

RESEARCH ARTICLE

A novel safety assurance method based on the compound equivalent modeling and iterate reduce particle-adaptive Kalman filtering for the unmanned aerial vehicle lithium ion batteries

Shunli Wang[1] | **Carlos Fernandez**[2] | **Yongcun Fan**[1] | **Juqiang Feng**[3] | **Chunmei Yu**[1] | **Kaifeng Huang**[3] | **Wei Xie**[4]

[1]Robot Technology Used for Special Environment Key Laboratory of Sichuan Province, Southwest University of Science and Technology, Mianyang, China

[2]Robert Gordon University, Aberdeen, UK

[3]School of Mechanical and Electrical Engineering, Huainan Normal University, Huainan, China

[4]Sichuan Huatai Electric Co., Ltd., Suining, China

Correspondence
Shunli Wang, Robot Technology Used for Special Environment Key Laboratory of Sichuan Province, Southwest University of Science and Technology, Mianyang 621010, China.
Email: 497420789@qq.com

Funding information
National Natural Science Foundation of China, Grant/Award Number: 61801407; Natural Science Foundation of Anhui Province of China, Grant/Award Number: KJ2019A0692 and KJ2017A458; Key Projects of Huainan Normal University, Grant/Award Number: 2018xj17zd; Sichuan Province Science and Technology Support Program, Grant/Award Number: 19ZDYF1098, 2019JDTD0019, 2019YFG0427 and 2018GZ0390; Scientific Research Fund of Sichuan, Grant/Award Number: 17ZB0453; Teaching Research Project, Grant/Award Number: 18lzx665, 18gjzx11 and 18xnsu12

Abstract

The safety assurance is very important for the unmanned aerial vehicle lithium ion batteries, in which the state of charge estimation is the basis of its energy management and safety protection. A new equivalent modeling method is proposed for the mathematical expression of different structural characteristics, and an improved reduce particle-adaptive Kalman filtering model is designed and built, in which the incorporate multiple featured information is absorbed to explore the optimal representation by abandoning the redundant and abnormal information. And then, the multiple parameter identification is investigated that has the ability of adapting the current varying conditions, according to which the hybrid pulse power characterization test is accommodated. As can be known from the experimental results, the polynomial fitting treatment is carried out by conducting the curve fitting treatment and the maximum estimation error of the closed-circuit-voltage is 0.48% and its state of charge estimation error is lower than 0.30% in the hybrid pulse power characterization test, which is also within 2.00% under complex current varying working conditions. The iterate calculation process is conducted for the unmanned aerial vehicle lithium ion batteries together with the compound equivalent modeling, realizing its adaptive power state estimation and safety protection effectively.

KEYWORDS

compound equivalent modeling, lithium ion batteries, reduce particle-adaptive Kalman filtering, state of charge estimation, unmanned aerial vehicle

1 | INTRODUCTION

The new energy promotion has already become a global consensus after its technology revolution and strategic adjustment, according to which the power supply issues attract great attention along with the continuous expansion of the energy development and utilization that becomes to be the main challenges. The lithium ion battery has the characteristics of high energy density, long life span, high output power, and excellent cost control, so thousands of them play an important role on the decontamination and emission reduction absolutely as well as the national economic progress.[1] The unmanned aerial vehicles (UAV) must meet three conditions: safety, cost-effective life cycle, and environmental friendship.[2] Nowadays, the lithium ion battery application has a large production capacity but its price is falling, which has become one of the development trends of new energy sources and applied in the unmanned aerial vehicles abundantly.[3] However, its safety protection problem is not solved yet due to the absence of its effective energy management, which should be overcome to accelerate its promotion and application.

The lithium ion battery is a complex electronic chemical system,[4-7] making it to be very hard to construct its equivalent model,[8] which affects the accuracy and reliability of the state estimation system.[9] At present, the development and application of the lithium ion battery enters a critical period as presentation, in which the competitive pressure is increasing on the high-end technology.[10] The key technologies should be broken for the equivalent modeling, in which the balance of complexity and precision is the main conundrum to be accomplished.[11,12] The state of charge is premise of all other battery state estimation that prevents abusing the battery energy in the complex working condition monitoring process,[11,13,14] which is also the basis of the ladder utilization for the battery accompanying in its whole life cycle span together with the overall performance optimization and accordance for its safety guarantee. Due to the existence of the process noise in the complex power supply working conditions, internal structures, environments, and measurement parameters, the feature information extraction and mathematical expression are difficult.[15] Therefore, the equivalent modeling is the key technology which bursts into the worldwide sight.[16]

The battery management system is a necessary part of the unmanned aerial vehicles that can be used as a long side, in which the equivalent circuit modeling is very important that affects its working performance, so it should be investigated and taken into account.[17] As the working characteristic of the lithium ion battery is nonlinear, its state of charge value should be estimated by the associated battery management system equipment, in which the accumulated estimation error should be avoided and reduced.[18] The energy management, charge-discharge control, overcharge, and overdischarge protection should be considered in the battery management system, the subsequences of which are proved accordingly. The equivalent circuit modeling is quite necessary that should be constructed in the lithium ion battery power supply applications.[19] Aiming to satisfy its working process simulation and mathematical expression targets as suspected, the equivalent circuit modeling should be constructed together with its effective parameter identification.[20] The safety modeling method was proposed to avoid the accumulated calculation error accused by the stable discharging platform of the lithium ion battery as before.[21] The equivalent modeling was analyzed that was adopted in the automated guided vehicle applications by the a lot of subsidies,[22] which was introduced into the accustomed Wiener continuous-time modeling process.[23] An enhanced equivalent circuit model was built accounting for the state of charge redistribution, state estimation, and temperature effect characterization, which had taken part in the working state monitoring process.[24] A novel parameter identification method was proposed to construct the equivalent circuit model considering its electrical properties and situations,[25] the characterization of which was evaluated for the lithium ion battery slurry with the bare 10-parameter equivalent model for the special damp conditions.[26] The electrical lithium ion battery model was built by considering the two-step procedure and parameter sensitivity, which was used in the tens of thousands power supply working conditions.[27] The model-based resistance estimation was conducted by using the electric vehicles operating data to overcome the application dam considering the multiple input parameters.[28] An easy-to-parameterize physics-informed battery model was built along with its application of the lithium ion battery diagnosis and degradation to avoid its damage.[29] The accurate power sharing method of the balanced battery state of charge was investigated in the distributed direct current micro-grid according to the cylinder barrel theory.[30] The interconnected observer was built for the concurrent estimation of the bulk and surface concentration in the lithium ion batteries.[31] The state of charge estimation was realized via the dual extended Kalman filter and the charging voltage curve,[32] and the comparative global optimization was conducted for the parameter identification of different equivalent circuit modeling algorithms.[33]

Meanwhile, the state estimation methods were investigated for its real-time working condition monitoring, which was conducted by using the capacity fade and internal resistance growth models.[34] The micro-short-circuit diagnosis was conducted basically for the series-connected lithium ion batteries by using the mean-difference model.[35] The model-based insulation fault diagnosis was conducted to overcome the safety protection barrier of electric vehicles.[36] The cycle life prediction was conducted for each battery cells in the aged lithium ion batteries by using the fad trajectory of the four-parameter model battling with its cyclic life.[37] The lump diffusion

lithium ion battery models were analyzed during the dynamic loads for the voltage prediction.[38] The model-based thermal runaway prediction was conducted from the kinetics analysis of the cell components bearing the temperature rise.[39,40] The quantitative validation of the calendar aging models was realized for lithium ion batteries,[41] and the model-based assessment of performance was realized by using the single ion conducting electrolytes.[42] The online thermal parameter estimation was investigated by using the coupled wide-temperature-range and electrothermal model,[43] on the basis of which a mechanism identification model-based state diagnosis was conducted for the energy storage system applications.[44] The state of charge estimation was conducted for the lithium ion batteries in electric vehicles,[45] the different ranges of which were analyzed in the aging mechanisms together with its multiple indicators.[46]

The model construction methods are analyzed that is based on the working principle and voltage characteristic analysis, aiming to protect the lithium ion battery in the cabin of the unmanned aerial vehicles. By combining the equivalent circuit model with different curve fitting structures, an improved compound equivalent modeling method is put forward to characterize the internal state of the lithium ion battery accurately including the cable resistance. It is then constructed by identifying the relevant undetermined coefficients, which is the basis of the subsequent state of charge estimation. Then, a novel capable reduce particle-adaptive Kalman filtering (RP-AKF) method is proposed and realized by the calculator, according to which the looped iterative calculation is put forward to realize the accurate state of charge estimation, which improves the parameter identification accuracy and adaptability effectively of the UAV lithium ion batteries.

2 | MATHEMATICAL ANALYSIS

The equivalent modeling construction method is investigated to ease the aeronautical auxiliary for the state of charge estimation, in which the inconsistency of the internal battery cells should be characterized to explore the accurate equivalent model construction. Various kinds of the equivalent models are analyzed and probed into their respective improvements. Considering the advantages of various methods, a compound equivalent modeling method is put forward and applied into the state of charge estimation of the UAV lithium ion batteries.

2.1 | Structural model building

The theoretical research and experimental verification are combined, in which the gradual and in-depth development of the equivalent model is established and the state estimation is realized with facility. The full life cycle equivalent modeling is realized for the lithium ion battery by considering the environmental and aging characteristics that are influenced by the bulk concentration. The input-output characteristics are considered fully under different environmental conditions by using the interconnected observer, in which the characteristics of temperature, aging and internal resistance factors are analyzed for the unmanned aerial vehicle lithium ion battery based on the data-driven strategies such as the single particle model and sliding mode observer. Combined with the equivalent circuit modeling and open-circuit-voltage characteristic analysis, the state of charge estimation model can be constructed that has the faculty of characterizing different working states and surface concentrations. As a result, the full life cycling equivalent model is built to realize the battery behavior characteristics and surface concentration. Furthermore, an adaptive parameter identification system is built that is suitable for the environmental changes and its online inner electrochemical sate estimation.

The state of charge estimation is investigated by the RP-AKF algorithm that is established for the lithium ion battery, in which the double-trackless transform closed-loop observer is constructed based on the density function. The time update and measurement state update are performed by the recursive feedback treatment to gain the high accuracy purpose, providing crucial messages for its effective energy management. Its weight distribution is performed according to the error gap between the predictive value and the prior value, according to which the state of charge values are observed and corrected in real time. The life cycle state of charge estimation and parameter correction are investigated by the iterate calculation modeling, aiming to insight into the commeasurable electrochemical states by the bulk and surface concentration. The battery model parameters are further calculated by using the estimation results, and the battery life cycle state estimation model is established on the basis of the multiple constraints. According to the estimation results, the relationship between aging, performance degradation, and internal parameters of the unmanned aerial vehicle lithium ion battery is gathered for its whole cycling charge-discharge lifespan. And then, the parameter correction strategy is optimized and introduced into the feature building modular process, the performance of which is verified under varying measurement noise and parametric uncertainties. Considering the research objectives, the theoretical model is designed together with its experimental verification as it is required in the complex working conditions of the power lithium ion batteries.

The overall phased objectives are determined by establishing the rational division, in which the research is carried out step by step by conducting the theoretical analysis. The model construction and the technical route are taken as follows. S1: The experimental study is conducted on the working

characteristics of the unmanned aerial vehicle lithium ion battery, in which the environmental influence factor can be obtained that is possible to be introduced into the iterate calculation process. Then, its behavior analysis is conducted on the lithium ion battery according to the cycling data at the battery dynamic working conditions accumulated in the previous time period, which provides an opportunity of substituting it into the correction stage.

S2: The equivalent model construction method is studied together with the state-space description of the external measurable parameters, which is used to accommodate the scarcity to the mathematical state-space description. By the full analysis of the temperature and aging characteristics, its mathematical expression is obtained by using the data-driven approach that is accommodated to interact through exchange in the iterate calculation process. The effective model is used to initialize the parameters by using the adaptive identification method to establish its state-space expression.

S3: The state of charge estimation method of the unmanned aerial vehicle lithium ion battery is verified by its embedded implementation to avoid the redundant repetition calculation, according to which the RP-AKF closed-loop observer is constructed. Then, the input parameters are assembled together in the designed battery management system test platform for the effective working state monitoring process.

S4: By analyzing the experimental results, the battery equivalent circuit model is constructed on the simulation and correction process, which is then used in the state of charge estimation of the unmanned aerial vehicle lithium ion batteries.

A full life cycled state of charge estimation with the correction strategy is established that is suitable for the multiple constraint conditions, according to which the assembling iterate calculation model is constructed for the iterate calculation process. The proposed method is verified by the online battery management system platform together with its gauges to further analyze the aging mechanism and the performance evolution of the unmanned aerial vehicle battery. The regularity and simultaneous update is then investigated for the modeling database, which is occupied with the state parameters.

2.2 | Equivalent circuit modeling

A full life cycle equivalent model is constructed aiming to characterize the behavior of the lithium ion battery at different working conditions by the data-driven algorithm with unusual data treatment, and its overall mathematical state-space expression is realized for the unmanned aerial vehicle lithium ion based on the equivalent circuit modeling and open-circuit-voltage characterizing treatment. Then, a parametric adaptive environmental change is introduced along with its aging mechanism analysis, the proposal of which covers all the important aspects in the state of charge estimation process and a complex equivalent circuit model is built together with its parameter identification.

The proposed model realizes the working process description by investigating the different effect simulation treatment of the unmanned aerial vehicle lithium ion batteries. In order to realize the mathematical description of the working characteristics, the shunt resistance is introduced into the model by the one-order resistance-capacitance (RC) equivalent modeling method combined its convenient calculation process and high accuracy expression. The series-connected resistances are introduced into the equivalent circuit model and mix it with the traditional equivalent modeling process, which is then connected to the parallel loop reverse diodes to characterize the charge-discharge resistance difference. As a result, it can realize the comprehensive and accurate working characterization of the lithium ion battery, in which the working characteristics are considered by combining the constructional optimization. According to the application condition characteristics of the lithium ion battery, the compound equivalent circuit modeling strategy is constructed that is improved from the original battery equivalent models, the structure of which is shown in Figure 1.

There are some parameters should be known in the above equivalent model. $E\ (t)$ characterizes the open-circuit-voltage value of the unmanned aerial vehicle lithium ion batteries. R_s is a big resistance that is wrapped up in a square dotted frame and R_o represents the Ohm resistance inside the battery. R_c is the additional resistance when the battery is in the charging process, while R_d represents the additional resistance inside the battery, which are used to characterize the internal difference in the batteries at

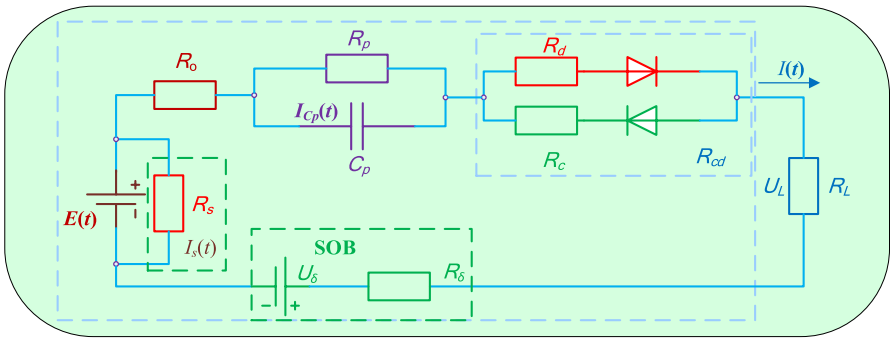

FIGURE 1 The compound equivalent battery model

time-varying working conditions. The proposed modeling method simulates the relaxation effects of the lithium ion battery by using the one-order RC network in order to realize its transient response characterization. R_p represents the polarization resistance, and C_p represents its polarization capacity. I_L represents the inflow and outflow current of the lithium ion battery when it is connected with the external circuit. An arbitrary linear independent source is connected with two RC networks which can be equivalent to a series-connected circuit of the voltage source and resistor. The model is constructed for the state characterization by using the resistance and capacitance, which is representative compared with other universal battery equivalent models. The closed-circuit-voltage value of the unmanned aerial vehicle lithium ion battery is indicated by conducting the intermittence discharging test, which represents the load voltage characteristic toward the current variation of the battery.

2.3 | State-space expression

The mathematical description is realized by considering the working characteristics and the parameter identification. As a result, the proposed integral approach is a mature state of charge estimation method without considering its internal complex chemical reaction. By the real-time parameter measurement, the remaining power can be monitored at any time, as the current acquisition accuracy is not high enough in the traditional methods.[47,48] When the initial value is not accurate, it will also affect the estimation error. Considering the energy dissipation efficiency in the charge-discharge Columbic on behalf of the lithium ion battery, the state of charge value has a close relationship with the current. Therefore, mounts of the battery factors should be considered, such as capacity, charge-discharge current, discharge frequency, and temperature change. To solve the above problem, an improved current integral method is introduced to estimate the state of charge value and applied into the RP-AKF calculation process, the calculation process of which is shown in Equation (1).

$$S(t) = \alpha \times S(0) \pm \frac{\int_0^t \eta_e \cdot I(t)dt}{\delta C_e}, t > 0 \quad (1)$$

where in $S(t)$ describes the SOC value at the time point of t, which is the combined value of its initial state value and its energy change during the power supply process of the lithium ion batteries. α is a time-varying correction factor of the capacity considering the equivalent Columbic efficiency of the self-discharge and cyclic aging characteristics, which is calculated by the initial open-circuit-voltage correction along with the real-time current time integral calculation. Through the differential expression analysis, the corrected value is defined as the final power state estimation result. By combining the unscented Kalman filtering and open-circuit-voltage correcting methods together, the state of charge estimation algorithm is realized in the micro-controller unit of STM32F103, which can maintain a good accuracy in the state of charge working state monitoring process and has good inhibition effect on the process noise.

The state-space representation is constructed for the equivalent circuit model, the mathematical description of which is described for the lithium ion battery. The parameter identification is constructed, in which the covariance and noise are generally considered as preowned conditions that are additionally considered in the dependent submodules. After establishing the state-space description structure, it is necessary to determine the coefficients in the iterate calculation process experimentally. And then, the parameter identification results are implemented in the separate modules, according to which a model is built for the battery state estimation, which is used for the parameter identification. Furthermore, the application characteristics and state estimation process of the battery are realized and the operating characteristics of the unmanned aerial vehicle battery can be developed by conducting the simulation experiments of the complex environmental working conditions. Afterward, the coefficients and their variation rules can be obtained through the parameter identification process, which are used to initialize the model factors. The mathematical representation and parameters are then analyzed to accommodate the lithium ion battery output features in different internal cascading cell states and an equivalent model is constructed to achieve the goal of working state monitoring framework construction. Furthermore, an effective state-space equation is constructed that is combined with experimental analysis and parameter identification.

2.4 | Adaptive correction

The proposed RP-AKF algorithm is used to correct the current value of the lithium battery state of charge by the error covariance correction while real-time online parameter measuring, which plays an adaptive power state adjustment role. The estimated state value is effectively corrected by updating the system noise together with its error covariance in real time. The error covariance matrix of the initial state is determined in advance, and the error covariance matrix is updated at the next time moment. And then, the Kalman gain is calculated according to the current error covariance, which is also used as the correction coefficient to the next calculation procedure. The state estimation value and the error covariance of the real-time power state values are estimated accordingly, based on which the mean and error covariance of the system noise and the process noise are updated continuously,

thereby realizing the state of charge estimation of the unmanned aerial vehicle lithium ion batteries.

The basic characteristic equations of the proposed RP-AKF calculation process are analyzed together with its operation order, which is based on the basic Kalman filtering strategies. The extension of this algorithm makes it suitable for the estimation of each environmental statement, which adds an adaptive effect based on the extended Kalman filter and the unscented Kalman filter so as to make the estimated value match the real value more closely. The iterate RP-AKF calculation method is used to estimate the state of charge of the lithium battery and also controls the covariance of the unknown noise in the algorithm, so that the final estimation effect is more stable when the working conditions are varying. At the same time, the interference of the noise on the estimation process is reduced effectively when estimating the state of charge value for the UAV lithium ion batteries.

The proposed RP-AKF algorithm uses the measurement data onto the filtering and estimation process, which determines whether the dynamic characteristics of the system change by the state of charge estimation model itself continuously. As a result, it estimates and corrects the model parameters and noise statistics to improve the filter structure by reducing the filtering error. This method combines the system identification and filtering estimation organically, in which the statistical properties of noise are introduced into the iterate calculation process. Through the measurement data, the mean and variance of the noise are estimated in real time, and then, the current state estimation value is corrected according to the mean and variance of the real-time update so as to improve the accuracy of the algorithm and avoid the divergence phenomenon. The mean value of the process noise and the measured noise is zero and its whole feature obeys the normal distribution, which are defined by Equation (2).

$$\begin{cases} w_k \sim N\left(q_k, Q_k\right) \\ v_k \sim N\left(r_k, R_k\right) \end{cases} \tag{2}$$

In Equation (2), k is a discrete time point. And then, the calculation process of the system noise estimator with high correlation quantity is realized for the experimental design as shown in Equation (3).

$$\begin{cases} q_{k+1} = \dfrac{1}{k+1} G \displaystyle\sum_{i=0}^{k} \left(\hat{x}_{k+1} - A\hat{x}_k - Bu_k\right) \\ Q_{k+1} = \dfrac{1}{k+1} G \displaystyle\sum_{i=0}^{k} \left(L_{k+1}\hat{y}_{k+1} y_{k+1}^T L_{k+1}^T + \hat{P}_{k+1} - AP_{k+1}A^T\right) G^T \\ \hat{r}_{k+1} = \dfrac{1}{k+1} \displaystyle\sum_{i=0}^{k} \left(y_{k+1} - C\hat{x}_{k+1|k}\right) \\ \hat{R}_{k+1} = \dfrac{1}{k+1} \displaystyle\sum_{i=0}^{k} \left(\bar{y}_{k+1}\bar{y}_{k+1}^T - CP_{k+1|k}C^T\right) \end{cases} \tag{3}$$

In Equation (3), "∧" indicates that the statistic of this special factor is an estimator. x_k is the system state at time k and y_k is an observation signal corresponding to the state of charge. u_k is the input of the system. A is a state transition matrix and B is the system control matrix. Meanwhile, G is the observation matrix, the value of which is set as $G = \left(\Gamma^T\Gamma\right)\Gamma^T$ by taking Γ as the noise drive matrix. The values obtained in the Equation (3) are the arithmetic mean values, which are the weighting coefficients of each term $(k+1)^{-1}$. In the time-varying system, the recent data have a great influence on the state of charge estimation process. Therefore, the estimator is improved by the exponential weighting method and each formula is multiplied by the different exponential weighting coefficient β, which satisfies the functional relationship as shown in Equation (4).

$$\beta_i = \beta_{i-1} b, \left(0 < b < 1, \sum_{i=0}^{k} \beta_i = 1\right) \tag{4}$$

Furthermore, the numerical calculations are used to obtain an iterative calculation expression as shown in Equation (5).

$$\beta_i = d_k b^i, \left(d_k = \frac{1-b}{1-b^{k+1}}, i = 0,1,2,3,\cdots,k\right) \tag{5}$$

In the Equation (5), b is a forgetting factor which is calculated by replacing each item of $(k+1)^{-1}$ in the original estimator with β_{k-1}, the noise estimation requirements of the improved time-varying system are obtained, according to which the specific steps of the designed calculation process are obtained. The first step is to realize the initialization of the parameters, in which the initial value x_0 of the system state and the covariance matrix P_0 of the initial state error are obtained as shown in Equation (6).

$$\hat{x}_0 = E\left[x_0\right], P_0 = E\left[\left(x_0 - \hat{x}_0\right)\left(x_0 - \hat{x}_0\right)^T\right] \tag{6}$$

After that, the state and error covariance matrix at time point $k+1$ can be calculated as shown in Equation (7).

$$\begin{cases} \hat{x}_{k+1|k} = A\hat{x}_k + Bu_k + \Gamma\hat{q}_k \\ P_{k+1|k} = AP_kA^T + \Gamma\hat{Q}_k\Gamma^T \end{cases} \tag{7}$$

Furthermore, the Kalman gain can be calculated according to the error covariance of the current state obtained in the previous step that is shown in Equation (8).

$$L_k = P_{k+1|k}C^T\left(CP_{k+1|k}C^T + R_k\right)^{-1} \tag{8}$$

Finally, according to the system observation value y_{k+1}, the estimated state value and its error covariance matrix at the next time moment are updated as shown in Equation (9).

$$\begin{cases} \hat{x}_{k+1} = \hat{x}_{k+1|k} + L_k \bar{y}_{k+1} \\ P_{k+1|k} = \left(E - L_k C\right) P_{k+1|k} \end{cases} \tag{9}$$

In Equation (9), E is a unit matrix. Further, the calculation process can return to the first step by updating q_k, r_k, Q_k, and R_k; accordingly, the iterative calculation is continued until it meets the requirement. The proposed RP-AKF method is suitable for the nonlinear discrete state of charge estimation systems, in which the complex working conditions and the noise statistical characteristics are changed drastically along with the actual working conditions. In order to avoid the divergence disks in the filtering and estimation process under complex conditions, the idea of proportional integral derivative control is introduced into the correcting stage in order to improve the state of charge estimation accuracy of the unmanned aerial vehicle lithium ion batteries based on the iterative calculation process, considering its high convergency advantages. The mathematical calculation of its introduced incremental control algorithm is shown in Equation (10).

$$\begin{cases} u_k = K_p \left[e_k + \beta \dfrac{T}{T_1} \displaystyle\sum_{j=0}^{k} e_j + \dfrac{T}{T_D} \left(e_k - e_{k-1}\right) \right] \\ \Delta u_k = u_k - u_{k-1} = K_p \left(e_k - e_{k-1}\right) + K_1 e_k + K_D e_k + K_D \left(e_k - 2e_{k-1} + e_{k+1}\right) \end{cases} \tag{10}$$

As can be known from the incremental calculation algorithm shown in Equation (10), the integral coefficient is set as $k_1 = k_p T/T_1$ which is used for the integral control link. U_k is used as the terminal output voltage of the lithium ion battery and e_k is taken as its time-varying power state. The differential coefficient is set as $k_D = k_p T_1/T$ which is used for the differential control and proportional coefficient calculation. k_p is the proportional coefficient of the proportional control coefficient. T is the system sampling time period, in which T_1 is the integral time coefficient and T_D is the differential practice coefficient. The incremental correction has a small amount of calculation, but it makes the operation integral to be accumulated with the larger control amount. Therefore, it is combined with the integral separation and used as the dead zone. In order to overcome the problems of low precision and low practicability in the state of charge estimation of power lithium batteries state of charge, the statistical characteristics of the process noise can be corrected online and its estimation accuracy is improved by introducing the proposed RP-AKF algorithm into the state of charge estimation process.

Combined with the compound equivalent circuit model, the RP-AKF algorithm is used to estimate the SOC value of the lithium battery, in which the ampere-time integration method is also used, the terminal voltages U_{p1} and U_{p2} of the two RC loops are selected as the state variables, and the battery terminal voltage is selected as the observation parameter. And then, the inner state parameter relationship can be obtained as shown in Equation (11).

$$\begin{bmatrix} S_{k+1} \\ S_{k+1}^{p1} \\ S_{k+1}^{p2} \end{bmatrix} = \begin{bmatrix} 1 & 0 & 0 \\ 0 & e^{-\Delta t/\tau_1} & 0 \\ 0 & 0 & e^{-\Delta t/\tau_2} \end{bmatrix} \begin{bmatrix} S_k \\ S_k^{p1} \\ S_k^{p2} \end{bmatrix} + \begin{bmatrix} -\Delta t/Q \\ R_{d1}\left(1 - e^{-\Delta t/\tau_1}\right) \\ R_{d2}\left(1 - e^{-\Delta t/\tau_2}\right) \end{bmatrix} i_k + \Gamma w_k \tag{11}$$

In Equation (11), Δt is the sampling time and Q is the rated capacity of the lithium ion battery. In the signal sampling process, it is often interfered by some unknown noise, including various noises from the outside world and the signal itself because of the sensor accuracy. After the discretization treatment, the linearization is combined with the noise effects; the state-space mathematical equations of the state of charge estimation process can be obtained as shown in (12).

$$\begin{cases} \hat{x}_k = A_{k-1} \hat{x}_{k-1} + B_{k-1} u_{k-1} + \Gamma q_{k-1} \\ P = A_k P_{k-1} A_k^T + \Gamma Q_{k-1} \Gamma^T \end{cases} \tag{12}$$

As can be known from Equation (12), the out-of-range values are collected, and these interferences are corrected adaptively by using the hardware filtering. This algorithm not only reduces the hardware costs, but also is easy to be implemented. The proposed adaptive Kalman filter method estimates the dynamic state from the measured data in real time, which estimates and corrects the statistical characteristics of the noise continuously, improving the state of charge estimation accuracy. The process noise covariance Q is used in the calculation process as well as the measurement noise covariance R, which are set to be constant in the running process of the algorithm. As the above two noise covariances are not accurate in the practical applications, it may lead to a certain cumulative error easily bringing in a divergence problem in the calculation process. Moreover, when dealing with the nonlinear state of charge estimation system with large dimensionality, it is easy to cause the nonpositive or semipositive definite phenomena of the noise covariance matrixes in the iterate calculation process, making the estimation model to diverge.

Only when the dynamic model and the linearization transformation are accurate enough, can the results obtained by the RP-AKF algorithm be effective and approximated to the real value. In addition, the traditional calculation algorithm has a defect that will cause the calculation process to be divergence during the running process if the assumed initial value and covariance have large errors. In order to solve the noise error problem, an adaptive filtering treatment is introduced into the calculation process, in which the system noise is filtered adaptively as well as the system state estimation.

The noise statistics are corrected continuously by the change of the measured data, according to which the filtering precision is improved and the influence of noise is reduced.

The discretization sampling period is $T_s = 1$s; $E[w_k] = q_k$ and $E[v_k] = r_k$ are the mean values of the process noise w_k and the measurement noise v_k, the variance values of which are $D[w_k] = Q_k\delta_{kj}$ and $D[v_k] = R_k\delta_{kj}$. In addition, the process noise and the measurement noise are uncorrelated, and the parameters of q_k, r_k, Q_k and R_k are unknown, which are introduced into the adaptive Kalman filtering calculation process to realize its accurate power state estimation. The unmanned aerial vehicle lithium battery state of charge estimation is realized by using the adaptive RP-AKF calculation. First of all, the parameters can be initialized at the time point of $k = 0$, and then, the initial estimated value of the power state and its error covariance are shown in Equation (13).

$$\hat{x}_0 = E\left[x_0\right], P_0 = E\left[\left(x_0 - \hat{x}_0\right)\left(x_0 - \hat{x}_0\right)^T\right] \tag{13}$$

Then, the state of the k-time uncertainty and the error covariance matrix are time-updated from the power state at $k-1$ time point together with its error covariance matrix, and the calculation process is obtained as shown in Equation (14).

$$\begin{cases} \hat{x}_k = A_{k-1}\hat{x}_{k-1} + B_{k-1}u_{k-1} + \Gamma q_{k-1} \\ P_k = A_k P_{k-1} A_k^T + \Gamma Q_k \Gamma^T \end{cases} \tag{14}$$

where in the matrix A^T is the transposed matrix of A. $\hat{x}_k$ and P_k are the priori estimation of the power state and its error covariance at time k, respectively. Afterward, the Kalman gain matrix K_k is obtained as shown in Equation (15).

$$K_k = P_k C_k^T \left(C_k P_k C_k^T + P_{k-1}\right)^{-1} \tag{15}$$

If the current state estimation uncertainty is high, P_k will become larger which will make K_k larger correspondingly, resulting in a bigger update state of the state of charge estimation system. In addition, if the ambient noise is large, P_{k-1} will become larger which will make K_k smaller. Furthermore, the measured data are used to update the estimated amount of the next time point state and the error covariance continuously, the expression of which is shown in Equation (16).

$$\begin{cases} \hat{x}_k = \hat{x}_{k|k-1} + \left[y_k - \left(C\hat{x}_{k|k-1} + Du_k + d - r_{k-1}\right)\right] \\ P_k = \left(E - K_k C_k\right) P_{k|k-1} \end{cases} \tag{16}$$

The state of charge estimation at the next time point is equal to the sum of the priori state estimation at that time moment mixed with a weighted correction term, among which E is the unit matrix. Due to the new information provided by the measured values, the state uncertainty is reduced continuously, that is, P_k is a decreasing process. At last, the measured data are used to estimate the mean and variance of the noise online continuously, and the estimated power state can be replaced with the updated state values to achieve the alternate update of the estimated state quantity considering the noise statistics, the mathematical expression of which is described as shown in Equation (17).

$$\begin{cases} q_k = \left(1 - d_{k-1}\right) q_{k-1} + d_{k-1} G\left(\hat{x}_k - A\hat{x}_{k-1} - Bu_{k-1}\right) \\ Q_k = \left(1 - d_{k-1}\right) Q_{k-1} + d_{k-1} G\left(L_k \hat{y}_k \hat{y}_k^T L_k^T + P_k - AP_{k|k-1}A^T\right) G^T \\ r_k = \left(1 - d_{k-1}\right) r_{k-1} + d_{k-1}\left(y_k - C\hat{x}_{k|k-1} - Du_{k-1} - d\right) \\ R_k = \left(1 - d_{k-1}\right) R_{k-1} + d_{k-1}\left(\hat{y}_k \hat{y}_k^T - CP_{k|k-1}C^T\right) \end{cases} \tag{17}$$

In the formula, the parameter values of G and d_{k-1} are set as $G = (\Gamma^T\Gamma)\Gamma^T$ and $d_{k-1} = (1-b)/(1-b^k)$, in which b is the forgetting factor ($0 < b < 1$) and set as $b = 0.96$. $\Gamma = [0.01\ 0.01]^T$. As can be known from the above analysis, q_k, r_k, Q_k, and R_k are estimated online in real time and the target of the state variable is corrected continuously in the state of charge estimation process so as to achieve the adaptive correction purpose, thereby improving its power state estimation accuracy. On the basis of Kalman filtering algorithm, the specific steps of the designed RP-AKF calculation algorithm are described as follows. The first step is the initialization process, in which the initial values of the power state and its covariance are set as shown in Equation (18).

$$\hat{x}_0 = E\left[x_0\right], P_0 = E\left[\left(x_0 - \hat{x}_0\right)\left(x_0 - \hat{x}_0\right)^T\right] \tag{18}$$

Next, the power state of the energy storage system at time k and its error covariance matrix are updated by conducting the correction strategies, the calculation process of which is described as shown in Equation (19).

$$\begin{cases} \hat{x}_{k|k-1} = A_{k-1}\hat{x}_{k-1|k-1} + B_{k-1}u_{k-1} \\ P_{k|k-1} = A_{k-1}P_{k-1|k-1}A_{k-1}^T + \Gamma_{k-1}Q_k\Gamma_{k-1}^T \end{cases} \tag{19}$$

Furthermore, the Kalman gain K_k is calculated accordingly from the error covariance matrix of the current state obtained in the previous step that is shown in the Equation (20).

$$K_k = P_{k|k-1}C_k^T\left(C_k P_{k|k-1} C_k^T + R_k\right)^{-1} \tag{20}$$

Then, the next time point estimated power state value and the error covariance matrix are updated and corrected according to the observation value of the power supply system as shown in the Equation (21).

$$\begin{cases} e_k = y_k - C_k\hat{x}_{k|k-1} - D_k u_k \\ \hat{x}_{k|k-1} = \hat{x}_{k|k-1} + K_k e_k \\ P_{k|k} = \left(I - K_k C_k\right) P_{k|k-1} \end{cases} \tag{21}$$

Finally, Q and R are updated by the previous calculated parameters, the calculation process of which is described as shown in Equation (22).

$$\begin{cases} Q_k = (1-d_{k-1})\, Q_{k-1} + d_{k-1} G \left(K_k \hat{y}_k \hat{y}_k^T L_k^T + P_k - A P_{k|k-1} A^T\right) G^T \\ R_k = (1-d_{k-1})\, R_{k-1} + d_{k-1} \left(\hat{y}_k \hat{y}_k^T - C P_{k|k-1} C^T\right) \end{cases} \tag{22}$$

On the basis of theoretical analysis and design, the power state iterate calculation algorithm is realized for the real-time power state estimation by the modeling and simulation of the adaptive Kalman filtering strategies together with the reduced particle optimization.

2.5 | Iterate calculation

As the improved RP-AKF closed-loop observer is constructed by using the probability density functions, the time and measurement state update treatments are performed through the recursive feedback correction. The weight coefficients are assigned according to the observation values and prior-state values, in which the state of charge values are observed in real time during each iterate calculation steps. According to the power state estimation modeling strategy, the mathematical results of the battery model parameters are further optimized by using the estimated results together with its correction treatment, according to which the state estimation method of the battery life cycle state can be established by using the multiple constraints. After then, the relationship between aging, performance degradation, and internal parameters are analyzed, and the state estimation of the whole life cycling process is established for the lithium ion batteries, according to which the state parameter correction strategy is optimized and realized for the real-time power state monitoring purpose.

The high robust correction strategy is used together with its power state optimization and improvement, in which the real-time correction of voltage signal detection is adopted for the complex current varying working conditions. Considering the coefficient variation and the voltage change rate, and the effective average cell voltage U_s is obtained by the functional calculation. And then, the obtained effective average cell voltage U_s is combined with the constructed composite equivalent RP-AKF approach and taken as the main. The functional relationship is fitted by the identified parameters and estimated by the functional relationship between open-circuit-voltage and state of charge, in which the state of charge value can be estimated firstly by using the battery terminal voltage at $k = 0$ after the start of the program. It is then calculated through the current time integral treatment to obtain the state of charge value at $k + 1$ time point by the end of next time point in the voltage current correction process.

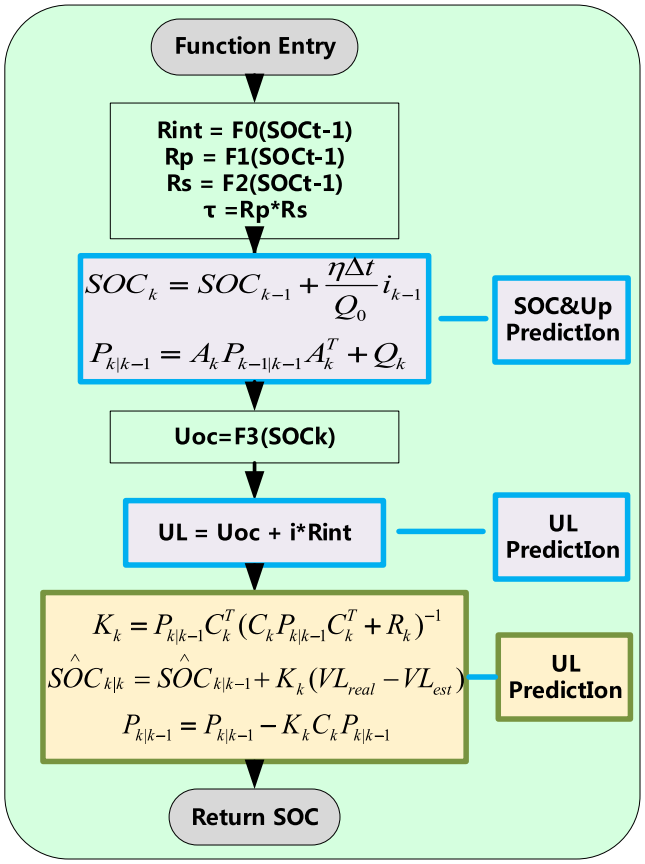

FIGURE 2 The state of charge estimation flowchart

Afterward, the terminal voltage error and filtering Kalman gain can be calculated by the modified mathematical power state estimation treatment after the correction treatment at the time point of $k + 1$ by the end of the voltage acquisition of actual value and estimated value computation according to the voltage error. Meanwhile, the output closed-circuit-voltage is estimated according to the real-time terminal voltage measurement and state of charge calculation. By looping the above iterate calculation process, the real-time online state of charge estimation is conducted and realized, the calculation process of which can be described as shown in Figure 2.

The software of the battery management system is designed for the unmanned aerial vehicle lithium ion batteries and the flow chart of its iterate power state calculation is programmed accordingly. By writing and debugging the program, the real-time parameter detection of the voltage and current is realized finally by the direct parameter measuring sensors together with the first in first out memory access. And then, the relevant reference data are used to complete the driver program of the digital temperature sensor. The temperature detection is also conducted, which is displayed through the liquid crystal display equipment, realizing the targeted functions of the battery management system for the power lithium ion batteries. The RP-AKF algorithm implements the real-time state of charge estimation, in the

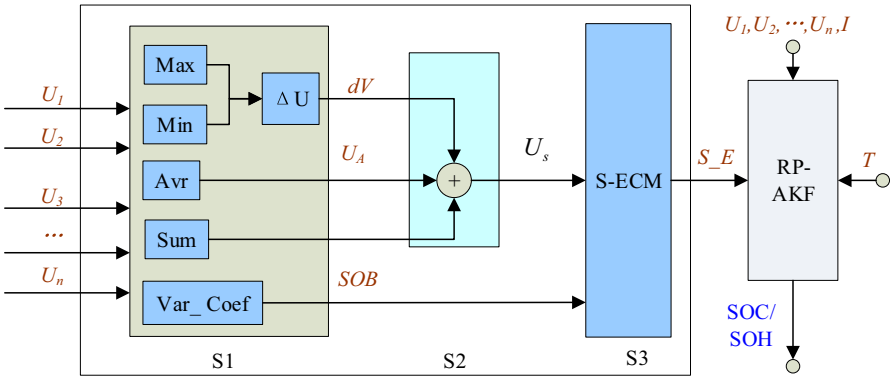

FIGURE 3 The real-time state of charge calculation model

equivalent modeling process of which the real-time detection of each cell voltage U_1, U_2, U_3,... and U_n and the current value I_L are taken into the calculation process under the influence of the operating conditions. Combined with the correction strategies, the power state estimation is realized by the iterate calculation process as shown in Figure 3.

The correction strategy is obtained for the influencing factors of the equivalent modeling process together with the random vector probability dynamics, which is combined with the theoretical and experimental analysis of the affecting factors, such as charge-discharge current, temperature change, working life, self-discharge rate, and cell-to-cell consistency. The characteristics are obtained by using the theoretical analysis combined with the operating experimental results, in which the unscented transform technique is used for the state equation and its covariance calculation. The overall modeling structure is designed to realize the adaptive online power state estimation, in which the inlet parameters are the individual cell voltages U_1, U_2, U_3,..., and U_n that are used as the main factors of the functional equations. The calculation process is optimized for the state estimation in the first part of the S1 step, in which U_A and dU is described by Equation (23).

$$\begin{cases} U_A = \dfrac{1}{n}\left(U_1 + U_2 + U_3 + \cdots + U_n\right) \\ U_{\max} = Max\left(U_{A1}, U_{A2}, U_{A3}, \cdots, U_{Am}\right) \\ U_{\min} = Min\left(U_{A1}, U_{A2}, U_{A3}, \cdots, U_{Am}\right) \\ dU = U_{\max} - U_{\min} \end{cases} \tag{23}$$

In Equation (23), n is the cell number of the lithium ion batteries, the parallel cells of which are expanded as a single battery cell. U_1, U_2, U_3,..., and U_n are the cell voltages. U_{A1}, U_{A2}, U_{A3},..., and U_{Am} are the average value of U_A obtained at the first m time points. Furthermore, the equilibrium state parameter state of balance (SOB) among the inner battery cells of the lithium ion battery pack can be obtained as shown in Equation (24).

$$\mathrm{SOB} = \theta^2 = \frac{1}{n}\sum_{i=1}^{n}\left(\frac{U_i - U_A}{U_A}\right)^2 \tag{24}$$

The mean value of the combined voltage are obtained in the S2 calculation step, in which the closed-circuit-voltage and the voltage difference are combined together to obtain the effective average voltage U_s. It is then substituted for the calculation of U_s as shown in Equation (25).

$$U_s = h\left(dU, U_A, U_L\right) \tag{25}$$

In Equation (25), $h(*)$ is a function of the effective mean voltage. And then, the input parameters are the measured individual cell voltage values of U_1, U_2, U_3,..., and U_n and the current value I_L, which are used in the S3 calculation process. The equilibrium state parameter is combined with the temperature and aging factor correction to construct the equivalent circuit model together with the mathematical description of its state-space equations. As a result, the information covered in the real-time detection signals can be mined, realizing the real-time effective state expression in combination with the signal change of the input parameters. To a certain extent, the adaptability of the algorithm is improved by adapting to the state of charge estimation model and analysis of the accurate power state estimation under different working conditions.

The mechanism in different conditions is used for the unmanned aerial vehicle battery modeling process, according to which the state of charge estimation model framework design is completed. The mathematical expressions of the strong nonlinear operating characteristics are explored, revealing the mechanism of the operating characteristics. Combined with the experimental analysis, the model parameters are proved along with piecewise linearization and can be obtained for the different dynamic groups, in which the mathematical description of the battery characteristics can be investigated in different working conditions. Through the looping iterative calculation process, the state of charge and ohmic resistance are estimated in real time and also used for the real-time working state characterization purpose, in which the initialization calculation is realized at the first stage by Equation (26).

$$\begin{cases} t=0, \hat{x}_0^+ = E\left(X_0^x\right), \hat{R}_{1,0}^+ = E\left(R_{1,0}\right) \\ P_{x_0}^+ = \sum_{i=0}^{2n} \omega_i^{(c)} \left(X_{0,i}^x - \hat{x}_0^+\right)\left(X_{0,i}^x - \hat{x}_0^+\right)^T \\ P_{R_{1,0}}^+ = E\left[\left(R_{1,0} - \hat{R}_{1,0}^+\right)\left(R_{1,0} - \hat{R}_{1,0}^+\right)^T\right] \end{cases} \tag{26}$$

And then, the measurement equation of the state of charge estimation system is obtained by using the idea of the adaptive Kalman filtering treatment that is shown in Equation (27).

$$\begin{cases} P_{x,t/t-1} = E\left[\left(x_t - \hat{x}_{t/t-1}\right)\left(x_t - \hat{x}_{t/t-1}\right)^T\right] = \sum_{i=0}^{2n} \omega_i^{(c)} \\ \left(X_{t/t-1,i}^x - \hat{x}_{t/t-1}\right)\left(X_{t/t-1,i}^x - \hat{x}_{t/t-1}\right)^T + Q \\ P_{xy,t} = \sum_{i=0}^{2n} \omega_i^{(c)} \left[X_{t/t-1,i}^x - \hat{x}_{t/t-1}\right]\left[y_{t/t-1,i} - \hat{y}_t\right]^T \\ P_{yy,t} = \sum_{i=0}^{2n} \omega_i^{(c)} \left[y_{t/t-1,i} - \hat{y}_t\right]\left[y_{t/t-1,i} - \hat{y}_t\right]^T + R \\ K_t = P_{xy,t} P_{yy,t}^{-1} \\ L_t^{R_1} = P_{R_{1,t}}^- C_t^{R_1} \left[C_t^{R_1} P_{R_{1,t}}^- \left(C_t^{R_1}\right)^T + \sigma_g\right]^{-1}. \end{cases} \tag{27}$$

And then, the unscented Kalman filter and extended Kalman filter algorithms are combined together in the proposed RP-AKF iterate calculation algorithm for the state of charge estimation in order to realize the co-estimation of the discharging capacity and the internal resistance at the same time. The noise model is obtained by the adaptive adjustment, and the state of charge value is estimated at the premise of the unknown process and observation noises, so that the estimation error is supposed to be very small. The varying range of the parameter covariance is managed to improve its stability and convergence, according to which the internal resistance values of the power lithium ion battery can be calculated accurately.

The intermittent aging degree measurement and the battery estimation model in the RP-AKF iterate calculation process are investigated to realize the real-time power state correction of the unmanned aerial vehicle lithium ion batteries. The experimental analysis is conducted in the charge-discharge maintenance, in which the model parameter principle is taken into consideration in the structural power state estimation process. According to the 1C discharging current rate experiments together with the ampere-hour integration treatment, the actual discharging electric quantity Q_n_Deter is obtained that is different from the current state together with the symbol S_n. The rated capacity Q_n_Rated is expressed with S_0. Furthermore, the relative change ratio δ_S in the current state is obtained, according to which the real-time state calculation is designed and realized as shown in Equation (28).

$$\begin{cases} K_Q = \delta_S = \dfrac{S_n}{S_0} \times 100\% = \dfrac{Q_n\_\text{Deter}}{Q_0\_\text{Rated}} \times 100\% \\ Q_n = K_Q Q_{n\_\text{Rated}} - \Delta Q_n, \Delta Q_n = f(N) \end{cases} \tag{28}$$

The equivalent modeling treatment is applied into the state-space description of the power lithium ion batteries and used for the real-time power state estimation, in which the aging process influence is characterized and the correction parameter is calculated to express the influence of the rated capacity. In order to realize the available capacity measurement target, the capacity correction coefficient ΔQ_n is calculated toward the superimposed cycling number of the rated capacity for the battery capacity varying characteristic description.

3 | EXPERIMENTAL ANALYSIS

The associated battery management system is designed and applied for different initial power conditions, parameter measuring accuracy together with the battery model equivalent model parameters, according to which the input factor influence effect analysis is carried out for the lithium ion batteries. The multiple current rate simulation conditions are combined with the changing law of the unmanned aerial vehicle working environments, according to which the experiments contain the different time-length combinations under normal conditions and the long-time discharging conditions. Furthermore, according to the complex time simulation conditions, the comparison of the estimation effects can be investigated under different noise influences and the reliable verification is realized finally together with the equivalent modeling effect.

3.1 | Test platform design

The charge-discharge current of the unmanned aerial vehicle lithium ion battery is not only an important external parameter to describe the working sate, but also an important factor of extended Kalman filter to realize the online state of charge estimation. The current detection methods include current transformer, Holzer induction principle, and serial resistance measuring approaches, and the current detection methods are compared in the experiments, according to which the electromagnetic current transformer is introduced into the battery management system which has the advantages of simple structure and long service life. As long as the sampling resistor is used and the voltage at the two ends of the sampling resistor is measured accurately, the charge-discharge current detection of the lithium ion battery can be

realized conveniently. The module hardware circuit of the battery management system is designed, in which the design and principle of the printed circuit board (PCB) drawing in Altium Designer (AD) software is investigated and then used to characterize the circuit components with welding and debugging convenience. After the hardware and software design and realization of the battery management system, the associated management equipment is designed and realized as shown in the left part of Figure 4.

According to the Holzer effect, the magnetic field produces to force perpendicular to the electron motion direction in the conductor when the current flowing through the conductor is in a magnetic field. It is gathered at the side of the electronic conductor, resulting in the conductor effect that is formed on both sides of the weak voltage difference. The Holzer current sensor is introduced for the current detection by using this principle, in which the current flows through the conductor that changes into a weak voltage signal. And then, the current detection can be realized by its real-time measurement, which has low power consumption and high accuracy. The resistance current is to be detected in the current loop in series with the precision resistor as the sampling resistor by measuring the voltage at both ends of the sampling resistance. Then, the current flows through the sampling resistor by the calculation of Ohm law at this time point in the loop circuit. The circuit is clear about structure, low in cost, good in real time, and high in accuracy, which has great influence on temperature and has no isolation effect that is easily disturbed by the ground pin. Compared with several current detection schemes, the series resistance current detection method has the simple circuit structure, high precision, low cost, and easy realization advantages, so it is used to detect the current with series resistance.

The open-circuit-voltage characteristics of the unmanned aerial vehicle lithium ion battery refer to the relationship between open-circuit-voltage and the battery remaining capacity parameter state of charge. The realization process is investigated by using the following experimental test. Firstly, the predischarge maintenance is conducted by using the $1C_5A$ discharging current rate until the voltage is up to the discharging end of voltage (EOV), the value of which is set as EOV = 2.75 V. It is then set static for 1.00 hour in order to make the internal interaction to be stable. Secondly, the unmanned aerial vehicle battery should be charged by using the constant-current charging mode with the current rate of $1C_5A$, the maintenance process of which will be stopped until the voltage is up to the end voltage limitation (EOV = 4.20 V). Thirdly, it should be discharged by using the constant-current discharging mode for half an hour by using the $0.10C_5A$ discharging current ratio. Fourthly, the experimental procedure is cycled for 20 operations.

The discrete points can be obtained to characterize the mathematical relationship between open-circuit-voltage and state of charge through the above experimental procedure changes, which can be obtained through the curve fitting method by the solid line that is shown in the right part of Figure 4. And then, the relationship between open-circuit-voltage and state of charge is obtained for the lithium ion battery. Meanwhile, the accurate mathematical model of the unmanned aerial vehicle lithium ion battery can be constructed, which is combined with the experimental HPPC test, in which the horizontal axis represents the state of charge value of the lithium ion battery and the vertical axis represents the open-circuit-voltage value.

The discrete point relationship between open-circuit-voltage and state of charge can be obtained through the intermittent discharging treatment of the lithium ion batteries, according to which the overall variation curve can be obtained by using the fitting acquisition method. Afterward, the typical unmanned aerial vehicle lithium ion batteries are selected as the experimental samples and the experiments are launched to obtain the performance characteristics through the voltage and current parameters by using the comprehensive operations of the multiple input factors. The dynamic experimental working state monitoring process of the lithium ion battery can be determined by using the comprehensive assessment of different working conditions, in which the accuracy of the simulation results can be verified by comparing the original nominal value with the experimental results. According to the experimental results, the dynamic estimation error of the lithium ion battery is less than 1.00%, which is obtained by comparing the experimental results with the original values. The polynomial fitting treatment is carried out by conducting the curve fitting method and the fitting error is 0.48%. The dynamic mathematical state-space equation can be obtained by the curve fitting treatment, according to which the changes with the three stages of steep and slow varying zones can be described mathematically.

3.2 | Multiple current rates

The unmanned aerial vehicle lithium ion battery is selected as the experimental object, and the test equipment is subsource BTS 750-200-100-4, the charge-discharge maximum power of which is 750 W with maximum current 100 A and maximum voltage 200 V. The charge-discharge experiments are carried out at different magnifications and the capacity test is performed, according to which the battery is fully charged by the phase charging process. Herein, the constant current is used to charge the battery at a current rate of 0.8 C (40 A) to 4.2 V, and then, the constant voltage 4.2 charge treatment should be investigated before it is less than 2.5 A. According to the above experimental treatment, it is considered that the unmanned aerial vehicle battery is charged fully, the charging process of which is shown in the left part of Figure 5.

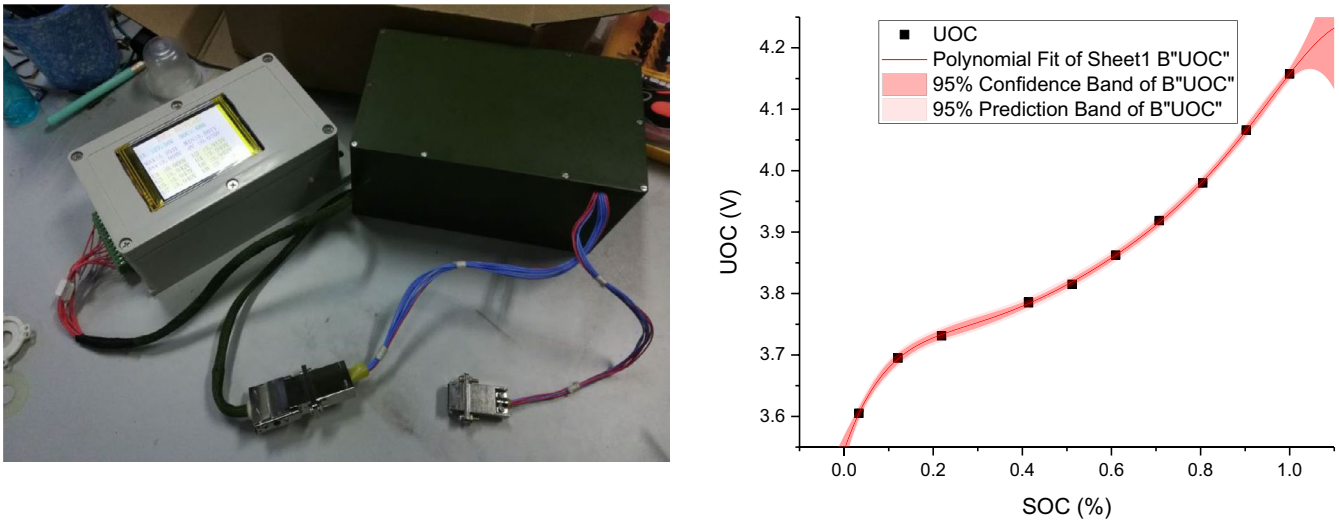

FIGURE 4 The battery management system and its open-circuit-voltage characteristics

In the Figure 5, U is the charging process voltage and I is the process current. After the charging maintenance is completed, the battery is set to stand for 1 hour and a constant-current discharge maintenance is performed at 1 C (50 A) to the cutoff voltage of 2.75 V, according to which the voltage vs time curve is obtained. The discharge experiments are then carried out in the same manner with the current rates of 0.8, 0.6, 0.4, and 0.2 C. The resulting voltage variation curve at different discharge rates is shown in the right part of Figure 5. As can be known from the experimental results, the voltage changes rapidly in the initial stage of the discharge process and the intermediate electric pressure changes slowly when it becomes an extremely high speed to the cutoff voltage. The discharge capacity of the battery is obtained in the case of 1, 0.8, 0.6, 0.4, 0.2 C, etc, the experimental result of the capacity variation along with different current rates can be obtained accordingly, in which the discharge capacity changes slightly and the overall discharge characteristics are large and the capacity is decreased in its overall changing trend. At the beginning of the battery discharge process, the voltage drops and the middle section is relatively flat, according to which the terminal phase drops rapidly.

3.3 | Parameter identification

A batch HPPC experiment is performed mainly from 0.1 to 1 to simulate its actual application, since the requirement for SOC < 0.1 is low and the test cannot be investigated when the pulse discharging voltage is lower than the limitation voltage value. During the period of 0.1-1, the experiment is performed once for every 0.1 capacity decrease treatment. The single HPPC experimental procedure in

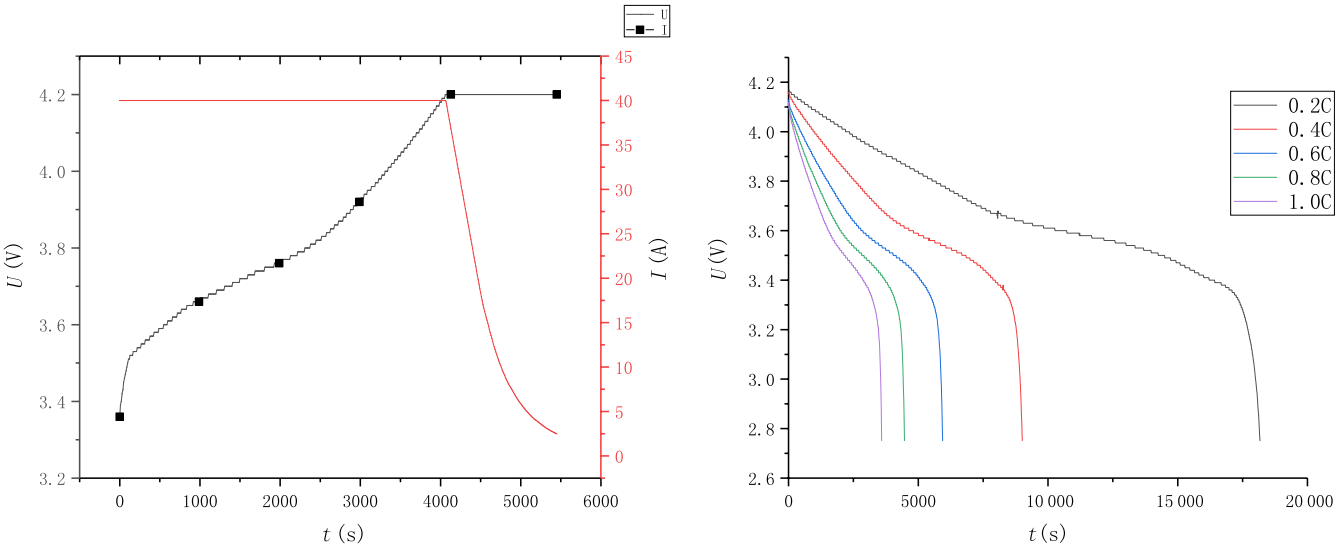

FIGURE 5 Different current rate charge-discharge curve

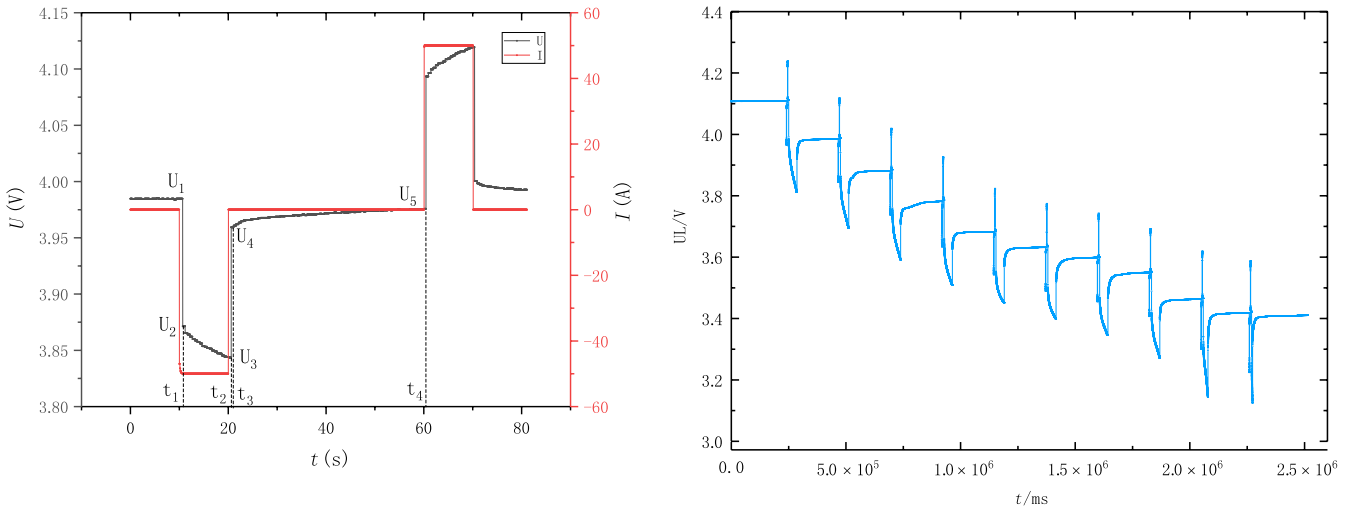

FIGURE 6 Single and complete HPPC test

every state of charge level is described as follows. Firstly, it is placed on hold and discharged at 50 A for 10 seconds, and then, it is left for 40 seconds. Afterward, it is charged at 50 A for 10 seconds and then set to be shelved again and the cycling charge-discharge test will be conducted until the HPPC experiment is completed. The experimental test data with SOC = 0.9 are described as shown in the left part of Figure 6.

The above figure is a graph showing the current and voltage data for the HPPC experiments with SOC = 0.9, in which t_1 is the time point when the voltage is U_2, t_2 is the time point of U_3, t_3 is the time point of U_4, and t_4 is the time point of U_5. There are 10 HPPC experimental tests that are performed sequentially from 0.1 to 1 and the overall experimental voltage change is shown in the right part of Figure 6. As the discharging current 50 A is large, the sudden discharge treatment has a large pressure drop. When discharging to SOC = 0.1447 in this experiment, the unmanned aerial vehicle battery voltage reaches the cutoff voltage of 2.75 V, so it cannot be discharged smoothly until the experiment is performed at SOC = 0.10 and the last test is performed at SOC = 0.1447 accordingly.

3.4 | Typical condition test

The typical condition test is applied, in which the working characteristics and the estimation effect are analyzed. The equivalent circuit model is established together with its parameter identification by using the experimental HPPC test data. In order to verify the validity of the proposed state of charge estimation model, the model data and actual data are compared and analyzed by investigating various working

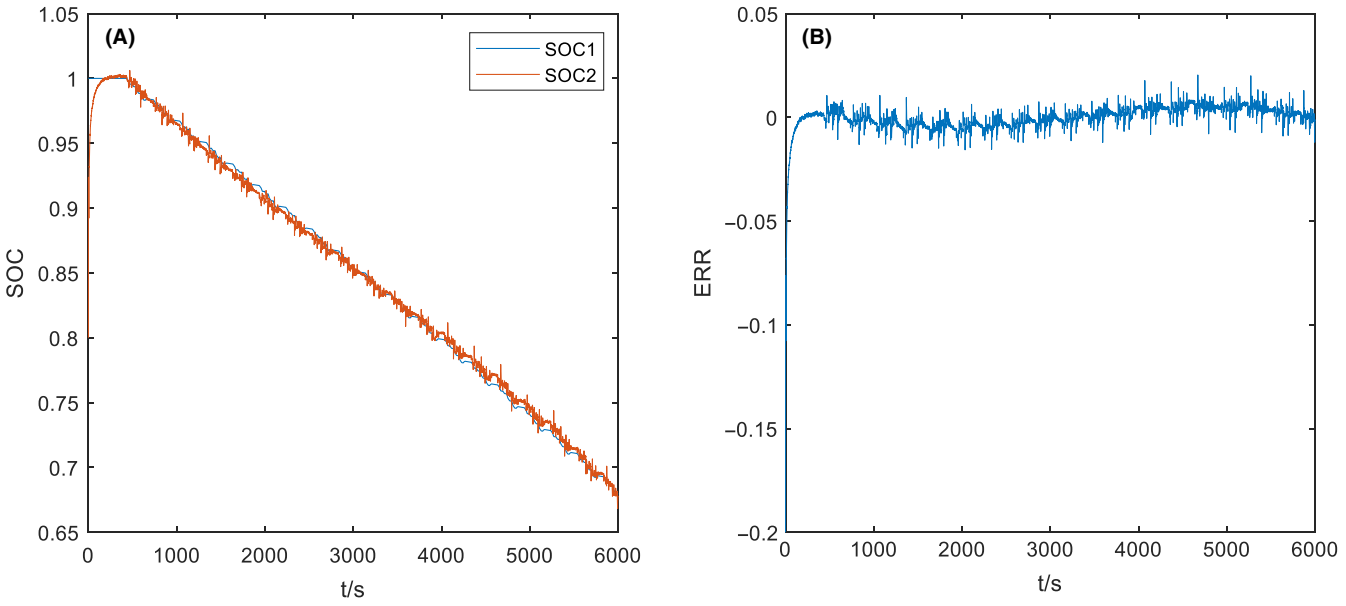

FIGURE 7 Power state estimation and error curve

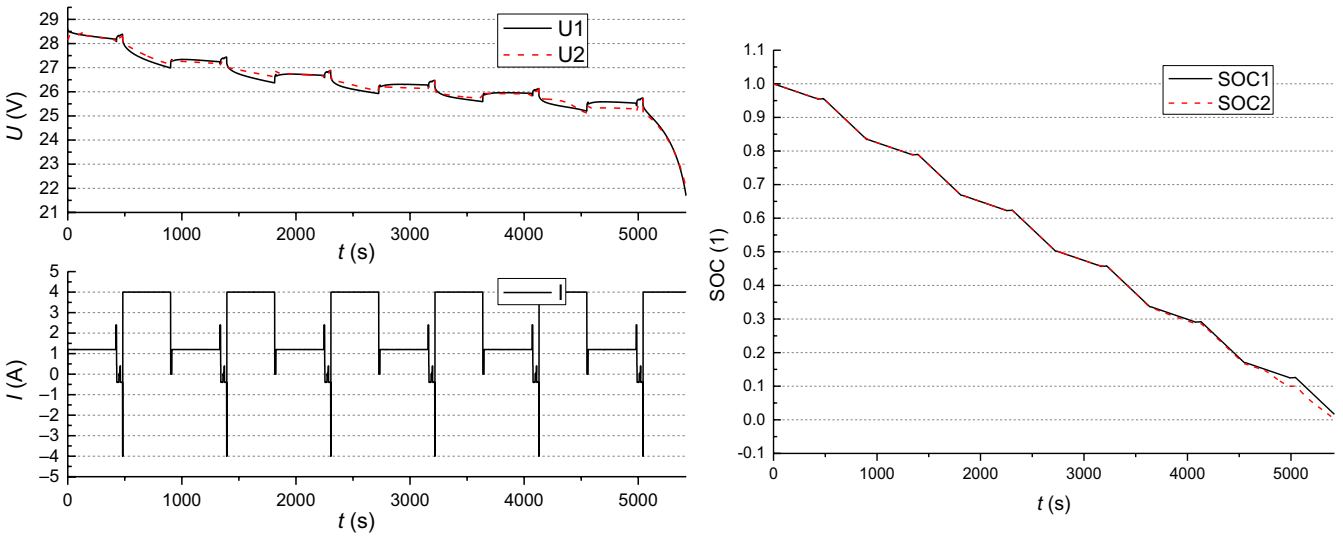

FIGURE 8 The closed-circuit-voltage tracking and state of charge estimation result

conditions of the unmanned aerial vehicle battery which are simulated by the constant and current varying pulse power discharge for a certain time period. The current value in the experimental data of the test equipment is used to obtain the estimated power state and its tracking output voltage by the simulation model which is then compared with the experimental acquisition terminal voltage. The experimental test is investigated and the initial state of charge error is given at least 20% in advance, so that the state of charge estimation is performed and its experimental results are described in Figure 7.

In Figure 7a, SOC1 is the true value and SOC2 is the estimated value using the proposed algorithm. Figure 7b is an error curve, in which the two states of charge value curves are intended to be subtracted. As can be known from the experimental results, the state of charge estimation error is less than 2.00%, in which the error of the initial value can be corrected very well and has a strong functional correction effect for the unmanned aerial vehicle lithium ion batteries.

3.5 | Complex current analysis

The high precision multimeter is used in the experiment, the resolution of which is five and a half. In the simulation condition, T_a is the meter to check the discharging time that is set to be 420 seconds; T_b is set to be 5 seconds and T_c is 20 seconds; T_d is set to be 10 seconds; T_e is 420 seconds. The tracking effect of closed-circuit-voltage along with the current change is analyzed for the simulated working condition. U1 and U2 represent the real-time sampling closed-circuit-voltage data, the changing curve of which is recorded for the unmanned aerial vehicle battery as time goes by. Through the experimental analysis, the comparison between the state of charge estimation and the ampere-hour integral calculation results is obtained under the complex current varying working conditions as shown in Figure 8.

The proposed algorithm can track the closed-circuit voltage effectively, and its state of charge estimation error is 2.00%, which has a good state of charge estimation effect compared with the experimental results from the references of.[49-52] In the iterative calculation process, since the external measurable signal parameters are affected by the accuracy of the sampling module, the power estimation errors will occur inevitably and the observation noise is unavoidable. Furthermore, the influence of different acquisition module accuracy results is verified under time-varying process noise influence together with the parameter measuring effect, in which the sampling precision is 1 mV and 1 mA, respectively, under the complex simulated unmanned aerial vehicle working conditions. The state of charge estimation effect is verified experimentally under the influence of observation noise that are set, respectively. The experimental results are obtained in observing the limited influence at the beginning of the simulated working conditions, which has good experimental results in the whole time period of the power supplying process.

4 | CONCLUSIONS

The online remaining power estimation of the drone is the weight with difficulty for the unmanned aerial vehicle lithium ion batteries which are analyzed by carrying out the verification experiments and its equivalent model parameters are identified based on the improved characterization of the power state and its output parameters. The charging-discharging test is carried out under different magnifications, according to which the unmanned aerial vehicle battery operating characteristics are obtained and a novel equivalent model is constructed for the lithium ion battery by the model

equivalence analysis. An improved reduce particle-adaptive Kalman filtering algorithm is put forward based on the compound equivalent circuit model for the state of charge estimation of the lithium ion batteries, the experimental results of which show that the has good estimation results under various working conditions. The state of charge estimation can be realized for the lithium ion batteries, in which the real-time parameter detection is realized for the closed-circuit-voltage, current and temperature. The state of charge power state estimation effect is analyzed through the model parameter identification, the working characteristics of which are described effectively and used in the experimental study of the unmanned aerial vehicle lithium ion batteries, providing a effective reference for its energy management process.

ACKNOWLEDGMENTS

This research was supported by National Natural Science Foundation of China (No. 61801407), Natural Science Foundation of Anhui Province of China (No. KJ2019A0692), the Natural Science Foundation for the Higher Education Institutions of Anhui Province of China (No. KJ2017A458) and Key Projects of Huainan Normal University (2018xj17zd), Sichuan Province Science and Technology Support Program (No. 19ZDYF1098, 2019JDTD0019, 2019YFG0427, 2018GZ0390), Scientific Research Fund of Sichuan (No. 17ZB0453), Teaching Research Project (18lzx665, 18gjzx11, 18xnsu12). The authors thank the sponsors.

ORCID

Shunli Wang https://orcid.org/0000-0003-0485-8082

REFERENCES

1. Zhou H, Zhou F, Xu L, Kong J, Yang Q. Thermal performance of cylindrical Lithium-ion battery thermal management system based on air distribution pipe. *Int J Heat Mass Transf*. 2019;131:984-998.
2. Martín-Martín L, Gastelurrutia J, Larraona GS, Antón R, del Portillo-Valdés L, Gil I. Optimization of thermal management systems for vertical elevation applications powered by lithium-ion batteries. *Appl Therm Eng*. 2019;147:155-166.
3. Bai F, Chen M, Song W, et al. Investigation of thermal management for lithium-ion pouch battery module based on phase change slurry and mini channel cooling plate. *Energy*. 2019;167:561-574.
4. Won IK, Kim DY, Hwang JH, Lee JH, Won CY. Lifetime management method of lithium-ion battery for energy storage system. *J Electr Eng Technol*. 2018;13(3):1173-1184.
5. Yang J, Xu X, Peng Y, Zhang J, Song P. Modeling and optimal energy management strategy for a catenary-battery-ultracapacitor based hybrid tramway. *Energy*. 2019;183:1123-1135.
6. Yang F, Song X, Xu F, Tsui K-L. State-of-charge estimation of lithium-ion batteries via long short-term memory network. *IEEE Access*. 2019;7:53792-53799.
7. Wang S-L, Shi J-Y, Fernandez C, Zou C-Y, Bai D-K, Li J-C. An improved packing equivalent circuit modeling method with the cell-to-cell consistency state evaluation of the internal connected lithium-ion batteries. *Energy Sci Eng*. 2019;7(2):546-556.
8. Chen L, Wang Z, Lu Z, et al. A novel state-of-charge estimation method of lithium-ion batteries combining the grey model and genetic algorithms. *IEEE Trans Power Electron*. 2018;33(10):8797-8807.
9. Wang X, Xie Y, Day R, et al. Performance analysis of a novel thermal management system with composite phase change material for a lithium-ion battery pack. *Energy*. 2018;156:154-168.
10. Saw LH, Poon HM, Thiam HS, et al. Novel thermal management system using mist cooling for lithium-ion battery packs. *Appl Energy*. 2018;223:146-158.
11. Tang X, Gao F, Zou C, Yao KE, Hu W, Wik T. Load-responsive model switching estimation for state of charge of lithium-ion batteries. *Appl Energy*. 2019;238:423-434.
12. Wang YJ, Sun ZD, Chen ZH. Development of energy management system based on a rule-based power distribution strategy for hybrid power sources. *Energy*. 2019;175:1055-1066.
13. Trovò A, Marini G, Sutto A, et al. Standby thermal model of a vanadium redox flow battery stack with crossover and shunt-current effects. *Appl Energy*. 2019;240:893-906.
14. von Lüders C, Keil J, Webersberger M, Jossen A. Modeling of lithium plating and lithium stripping in lithium-ion batteries. *J Power Sources*. 2019;414:41-47.
15. Mandli AR, Ramachandran S, Khandelwal A, Kim KY, Hariharan KS. Fast computational framework for optimal life management of lithium ion batteries. *Int J Energy Res*. 2018;42(5):1973-1982.
16. Chen C, Xiong R, Shen WX. A lithium-ion battery-in-the-loop approach to test and validate multiscale dual H infinity filters for state-of-charge and capacity estimation. *IEEE Trans Power Electron*. 2018;33(1):332-342.
17. Liu K, Li K, Ma H, Zhang J, Peng Q. Multi-objective optimization of charging patterns for lithium-ion battery management. *Energy Convers Manag*. 2018;159:151-162.
18. He F, Li X, Zhang G, Zhong G, He J. Experimental investigation of thermal management system for lithium ion batteries module with coupling effect by heat sheets and phase change materials. *Int J Energy Res*. 2018;42(10):3279-3288.
19. Carkhuff BG, Demirev PA, Srinivasan R. Impedance-based battery management system for safety monitoring of lithium-ion batteries. *IEEE Trans Ind Electron*. 2018;65(8):6497-6504.
20. Berrueta A, Heck M, Jantsch M, Ursúa A, Sanchis P. Combined dynamic programming and region-elimination technique algorithm for optimal sizing and management of lithium-ion batteries for photovoltaic plants. *Appl Energy*. 2018;228:1-11.
21. Chen Z, Sun H, Dong G, Wei J, Wu JI. Particle filter-based state of charge estimation and remaining-dischargeable-time prediction method for lithium-ion batteries. *J Power Sources*. 2019;414:158-166.
22. Liu XY, Li WL, Zhou AG. PNGV equivalent circuit model and SOC estimation algorithm for lithium battery pack adopted in AGV vehicle. *IEEE Access*. 2018;6:23639-23647.
23. Wang XY, Wei XZ, Dai HF. Estimation of state of health of lithium-ion batteries based on charge transfer resistance considering different temperature and state of charge. *J Energy Storage*. 2019;21:618-631.
24. Bahramipanah M, Torregrossa D, Cherkaoui R, Paolone M. Enhanced equivalent electrical circuit model of lithium-based batteries accounting for charge redistribution, state-of-health, and temperature effects. *IEEE Trans Transp Electr*. 2017;3(3):589-599.

25. Zhang XI, Lu J, Yuan S, Yang J, Zhou X. A novel method for identification of lithium-ion battery equivalent circuit model parameters considering electrochemical properties. *J Power Sources*. 2017;345:21-29.
26. Wang Z, Zhao T, Yao J, Kishikawa Y, Takei M. Evaluation of the electrochemical characterizations of lithium-ion battery (LIB) slurry with 10-parameter electrical equivalent circuit (EEC). *J Electrochem Soc*. 2017;164(2):A8-A17.
27. Jin N, Danilov DL, Van den Hof PMJ, Donkers M. Parameter estimation of an electrochemistry-based lithium-ion battery model using a two-step procedure and a parameter sensitivity analysis. *Int J Energy Res*. 2018;42(7):2417-2430.
28. Lipu MSH, Hannan MA, Hussain A, et al. A review of state of health and remaining useful life estimation methods for lithium-ion battery in electric vehicles: challenges and recommendations. *J Clean Prod*. 2018;205:115-133.
29. Zhao LH, Liu ZY, Ji GH. Lithium-ion battery state of charge estimation with model parameters adaptation using H-infinity, extended Kalman filter. *Control Eng Pract*. 2018;81:114-128.
30. Hoang KD, Lee HH. Accurate power sharing with balanced battery state of charge in distributed DC microgrid. *IEEE Trans Ind Electron*. 2019;66(3):1883-1893.
31. Allam A, Onori S. An interconnected observer for concurrent estimation of bulk and surface concentration in the cathode and anode of a lithium-ion battery. *IEEE Trans Ind Electron*. 2018;65(9):7311-7321.
32. Wang L, Lu D, Liu Q, Liu L, Zhao X. State of charge estimation for LiFePO4 battery via dual extended kalman filter and charging voltage curve. *Electrochim Acta*. 2019;296:1009-1017.
33. Hu X, Yuan H, Zou C, Li Z, Zhang L. Co-estimation of state of charge and state of health for lithium-ion batteries based on fractional-order calculus. *IEEE Trans Veh Technol*. 2018;67(11):10319-10329.
34. Guha A, Patra A. State of health estimation of lithium-ion batteries using capacity fade and internal resistance growth models. *IEEE Trans Transp Electr*. 2018;4(1):135-146.
35. Guo F, Hu GD, Hong R. A parameter adaptive method with dead zone for state of charge and parameter estimation of lithium-ion batteries. *J Power Sources*. 2018;402:174-182.
36. Wang Y, Tian J, Chen Z, Liu X. Model based insulation fault diagnosis for lithium-ion battery pack in electric vehicles. *Measurement*. 2019;131:443-451.
37. Li JF, Lin CH, Chen KC. Cycle life prediction of aged lithium-ion batteries from the fading trajectory of a four-parameter model. *J Electrochem Soc*. 2018;165(16):A3634-A3641.
38. Ekstrom H, Fridholm B, Lindbergh G. Comparison of lumped diffusion models for voltage prediction of a lithium-ion battery cell during dynamic loads. *J Power Sources*. 2018;402:296-300.
39. Shukla V, Jena NK, Naqvi SR, Luo W, Ahuja R. Modelling high-performing batteries with Mxenes: the case of S-functionalized two-dimensional nitride Mxene electrode. *Nano Energy*. 2019;58:877-885.
40. Ren H, Zhao Y, Chen S, Wang T. Design and implementation of a battery management system with active charge balance based on the SOC and SOH online estimation. *Energy*. 2019;166:908-917.
41. Meng J, Cai L, Luo G, Stroe D-I, Teodorescu R. Lithium-ion battery state of health estimation with short-term current pulse test and support vector machine. *Microelectron Reliab*. 2018;88–90:1216-1220.
42. Wolff N, Roder F, Krewer U. Model based assessment of performance of lithium-ion batteries using single ion conducting electrolytes. *Electrochim Acta*. 2018;284:639-646.
43. Zheng L, Zhu J, Wang G, Lu D-C, He T. Differential voltage analysis based state of charge estimation methods for lithium-ion batteries using extended Kalman filter and particle filter. *Energy*. 2018;158:1028-1037.
44. Park J, Lee B, Jung DY, Kim DH. Battery state estimation algorithm for high-capacity lithium secondary battery for EVs considering temperature change characteristics. *J Electr Eng Technol*. 2018;13(5):1927-1934.
45. Shen P, Ouyang M, Lu L, Li J, Feng X. The co-estimation of state of charge, state of health, and state of function for lithium-ion batteries in electric vehicles. *IEEE Trans Veh Technol*. 2018;67(1):92-103.
46. Wang SL, Yu CM, Fernandez C, Chen MJ, Li GL, Liu XH. Adaptive state-of-charge estimation method for an aeronautical lithium-ion battery pack based on a reduced particle-unscented kalman filter. *J Power Electron*. 2018;18(4):1127-1139.
47. Couto LD, Schorsch J, Job N, Léonard A, Kinnaert M. State of health estimation for lithium ion batteries based on an equivalent-hydraulic model: an iron phosphate application. *J Energy Storage*. 2019;21:259-271.
48. Saxena S, Xing Y, Kwon D, Pecht M. Accelerated degradation model for C-rate loading of lithium-ion batteries. *Int J Electr Power Energy Syst*. 2019;107:438-445.
49. Zheng Y, Gao W, Ouyang M, Lu L, Zhou L, Han X. State-of-charge inconsistency estimation of lithium-ion battery pack using mean-difference model and extended Kalman filter. *J Power Sources*. 2018;383:50-58.
50. Ye M, Song X, Xiong R, Sun F. A novel dynamic performance analysis and evaluation model of series-parallel connected battery pack for electric vehicles. *IEEE Access*. 2019;7:14256-14265.
51. Tang X, Wang Y, Zou C, Yao KE, Xia Y, Gao F. A novel framework for lithium-ion battery modeling considering uncertainties of temperature and aging. *Energy Convers Manag*. 2019;180:162-170.
52. Sierra G, Orchard M, Goebel K, Kulkarni C. Battery health management for small-size rotary-wing electric unmanned aerial vehicles: an efficient approach for constrained computing platforms. *Reliab Eng Syst Safe*. 2019;182:166-178.

How to cite this article: Wang S, Fernandez C, Fan Y, et al. A novel safety assurance method based on the compound equivalent modeling and iterate reduce particle-adaptive Kalman filtering for the unmanned aerial vehicle lithium ion batteries. *Energy Sci Eng*. 2020;8:1484–1500. https://doi.org/10.1002/ese3.606